ELSEVIER

Journal of Alloys and Compounds 408–412 (2006) 1096–1102

Journal of ALLOYS AND COMPOUNDS

www.elsevier.com/locate/jallcom

Insights into the redox properties of ceria-based oxides and their implications in catalysis

Eleonora Aneggi, Marta Boaro, Carla de Leitenburg, Giuliano Dolcetti, Alessandro Trovarelli *

Dipartimento di Scienze e Tecnologie Chimiche, Università di Udine, Via Cotonificio 108, 33100 Udine, Italy

Received 30 July 2004; received in revised form 15 December 2004; accepted 15 December 2004
Available online 29 June 2005

Abstract

In the present work, the redox properties of ceria and related materials will be considered with a focus on these effects that are relevant in catalysis. Particularly, after briefly pointing out the relevant redox chemistry and characterization of ceria in classical TWC application, we will describe how the reduction/oxidation characteristics of ceria are of help in other applications, like the development of advanced ceria–zirconia based catalyst for auto exhaust treatment, and the elimination of soot from diesel engine exhaust. In the first example, different catalyst formulations based on ceria and zirconia are examined to see how catalytic activity is related with composition and a simple redox mechanism model for CO oxidation is also derived. A similar approach is used to characterize the role of ceria in the combustion of soot.

Keywords: Ceria; CeO_2; Ceria–zirconia; Temperature programmed reduction; Three-way catalysts; Redox behaviour; CO oxidation; Soot oxidation; Oxygen storage capacity

1. Introduction

The use of ceria and ceria-based materials in catalytic science is well established [1,2]. Ceria is presently used in a large number of industrial processes and it accounts for a large part of the rare earth oxide market [3]; undoubtedly its major commercial application is in the treatment of emissions from internal combustion engines where ceria-based materials have been used in the past 25 years [4]. The reason for the successful use of ceria in catalysis and especially in three-way catalysts (TWCs) has been discussed in detail in several review papers [5–7], and it is connected to its ability to undergo easy, fast, and reversible reduction to substoichiometric phases. Its more important action in TWCs is to take up and release oxygen following variations in the stoichiometric composition of the feedstream. When doing this, ceria is continuously and rapidly subjected to reduction and oxidation cycles with its oxygen composition alternating between CeO_2 and CeO_{2-x}. This function is called oxygen storage/release capacity or more generally it is referred to as *redox behaviour* which accounts for all the characteristics of the reduction and oxidation processes of CeO_2.

The dynamics controlling the redox properties of ceria is rather complex and several investigations have been carried out in the last years trying to understand the most important factors affecting the reduction process of ceria [8–14]. In this review, we will briefly describe the reduction properties of ceria and ceria-based materials and discuss their effect in catalysis by showing a few examples from our recent work. We will mainly focus on the characteristics of bare supports without including specifically the effects of noble metals.

2. The reduction behaviour under H_2-TPR conditions

2.1. Characteristics of ceria reduction

The reduction behaviour of CeO_2 (in pure and doped ceria) has been studied in detail using several techniques. A

* Corresponding author. Tel.: +39 0432558855; fax: +39 0432558803.
E-mail address: trovarelli@uniud.it (A. Trovarelli).

0925-8388/$ – see front matter © 2005 Elsevier B.V. All rights reserved.
doi:10.1016/j.jallcom.2004.12.113

large amount of information on the redox features has been collected by studying the interaction of ceria with H_2 and other probe molecules by temperature programmed reduction (TPR) [5,14].

TPR is a simple and quite useful method to obtain information on the steps involved in the reduction processes and, although it has several limitations that must be taken into account [15], it still remains a major characterization tool for these materials. The ability of ceria to be easily reduced to nonstoichiometric oxides is related to the properties of fluorite structured-mixed valence oxides to deviate from stoichiometry [16]. Reduction of CeO_2 is generally thought to occur via a stepwise mechanism, first reduction of the outer most layers of Ce^{4+} (surface reduction), then reduction of the inner Ce^{4+} layer (bulk reduction) at higher temperatures. A few mechanisms have been put forward to account for this behaviour that comprises sequential steps of: (i) dissociation of chemisorbed hydrogen with formation of OH groups; (ii) formation of anionic vacancies with desorption of water by recombination of −H and −OH (with concomitant reduction of Ce^{4+} to Ce^{3+}) and (iii) diffusion of surface anionic vacancies into the bulk [13,17]. This picture is consistent with the TPR profile of high surface area CeO_2, which shows two well-defined peaks centered at approximately 770 and 1100 K [15]. With low surface area ceria, reduction at low temperatures is negligible and only one peak due to bulk Ce^{4+} reduction is observed.

We have recently critically revised the two step model by developing a simple quantitative representation for the TPR profile of ceria which can explain the origin of the two different peaks in the reduction traces, suggesting the participation of small and large ceria crystallites in the reduction process at low and high temperature, respectively, and taking into account also textural modifications occurring during TP analysis [18,19]. It was shown that the TPR profiles can be modelled by assuming a surface kinetic control over the entire temperature range. By taking into account, the available data on oxygen diffusion coefficients we concluded that the TPR profile in ceria is not controlled by diffusion rate. Critical factors were the kinetics and the thermodynamics of reduction of small and large crystallites present in ceria samples. The bimodal peak shape of ceria is a consequence of the fact that nanocrystalline and bulk ceria possess different kinetic and thermodynamic properties. The equilibrium degree of reduction of nanocrystalline ceria indicates that reduction is complete at lower temperature owing to a lower reduction enthalpy [20]. Under this hypothesis, the profile of ceria reduction can be interpreted as follows: smaller ceria crystallites start to be reduced at low temperature (T, ca. 500 K) and can be reduced thermodynamically to a high degree even at these temperatures. Limitation in the degree of reduction is therefore given by the kinetic of the process (either dissociation of chemisorbed hydrogen or formation of surface anionic vacancies) and by the growth of ceria crystallites. Consumption of H_2 due to this process is responsible for the occurrence of the first peak. The consequence is that the shape

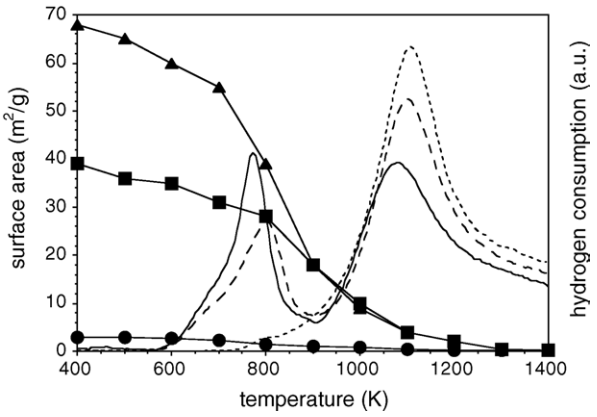

Fig. 1. Experimental TPR profile (right) and surface area drop (left) of three different samples of ceria: high-surface area (▲, —), medium surface area (■, - - -), low surface area (●, · · · · · ·).

of the first peak is related to the effect of balance between the dynamics of sintering (i.e. surface area loss) and the kinetic limitation for the reduction of nanocrystallites. At the same time, on increasing temperature, the material undergoes morphological modifications and small crystallites progressively modify to bulk ceria which has different kinetic and equilibrium reduction properties. At the temperature of ca. 900 K (i.e. in the middle between the two TPR peaks), the surface area drop indicates that we have mainly large ceria crystallites and therefore their reduction profile is similar to that observed for low surface area ceria which is reduced at higher temperatures. Fig. 1 highlights the relations between surface area and TPR profile.

2.2. Characteristics of ceria–zirconia reduction

One of the major breakthroughs in three-way catalysis was the introduction of modified ceria in the catalyst formulation. The incorporation of isovalent non-reducible elements like Zr^{4+} into CeO_2 lattice has been shown to strongly affect the redox properties of ceria by increasing its oxygen storage [21,22]. The presence of Zr modifies the reduction profiles of CeO_2 by decreasing the reduction temperature of Ce^{4+} by several degrees, depending on composition, and by increasing the total amount of reduced cerium.

Several important features characterize the redox profile of ceria–zirconia: (i) the extent of reduction is not strongly dependent on surface area, as it is similar for samples having 1–2 or 70–90 m^2/g; (ii) maximum reduction capabilities are observed in the intermediate composition range and (iii) over almost the entire range of compositions, mixed oxides are superior to pure ceria.

In the case of ceria–zirconia, in contrast with pure ceria, the electronic conductivity and activation energy for oxygen diffusion is similar in both nanocrystalline and sintered, bulk material [23]. It appears reasonable therefore to extend the above model also to the reduction of ceria–zirconia mate-

rials to explain the similar reduction behaviour shown by low and high surface area samples. The typical TPR profile consisting of one major peak in both low and high surface area sample can therefore be rationalized by the fact that thermodynamic reduction features of small and large ceria–zirconia crystallites are similar, and textural modifications under TPR analysis "does not" significantly affect TPR profile. This of course, represent an oversimplification since TPR profiles in ceria–zirconia are more complex than those of ceria and are strongly affected by compositional heterogeneities, sample pre-treatment and even sintering under different atmospheres [24]. We will return later on the intimate reasons why ceria–zirconia is more redox active than ceria.

3. Reduction behaviour under fast redox conditions

It is worth pointing out that the results provided by TPR analysis are strictly related to operating conditions under temperature variation mode and cannot represent the case of fast redox cycling experiments. In these cases, the reduction occurs in a short time (frequency of 1 Hz as an order of magnitude) and diffusion could be, and probably is, rate limiting, depending on temperature.

Generally, two different types of redox measurements can be distinguished [15]: (i) the measurement of total reduction capacity of a material (total or thermodynamic OSC), that is the total amount of oxygen that can be extracted from the solid at a certain temperature and (ii) the measurement of the most reactive and readily available oxygen only, that is, the fast, dynamic or kinetic OSC. In principle, there is no correlation between the two experiments, as one is associated to the total reducibility and is therefore a measurement carried out under thermodynamic equilibrium, while the other is a measure of the rate at which the oxygen comes out from the material, and as such correlated to the kinetics of reduction. To clearly see the difference, we can look at Fig. 2 where some TGA profiles are reported showing the weight loss of samples of $Ce_{0.5}Zr_{0.5}O_2$ against time under a H_2/N_2 atmosphere at 773 K [25]. The weight loss is due to abstraction of oxygen with formation of water. Total oxygen extracted can be calculated from the steady state portion of the curve, while the rate of oxygen release is proportional to the slope of the curve. Indeed there is no correlation between the two quantities. In the specific case, the rate is proportional to surface area of the sample while the total OSC is correlated to more subtle structural features (see below). TPR analysis lies in the middle between these two measurements, as in almost all the temperature range it is controlled by kinetics, but the overall H_2 consumption at high temperature is close to thermodynamics. Therefore, sometimes H_2 consumption values extracted from TPR are considered as total OSC.

The measurement of reduction properties under fast cycling feed conditions is generally carried out by feeding

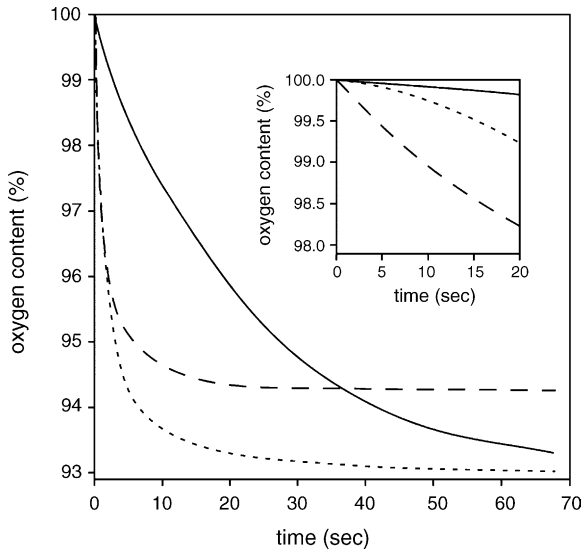

Fig. 2. Weight loss of samples of $Ce_{0.5}Zr_{0.5}O_2$ treated under H_2/N_2 atmosphere: sample 1, SA 1 m^2/g (—); sample 2, SA 20 m^2/g (· · · · · ·); sample 3, SA 50 m^2/g (- - - -) Ref. [25].

alternately to the catalyst pulses of reducing and oxidizing mixtures (typically CO or H_2 as reducing agents and O_2 or H_2O as oxidant) at a predetermined frequency. Although these methodologies are much better related to the operation of catalysts under real TWC conditions, running dynamic OSC experiments under simulated conditions involves several different variables and the comparison of experiments from different laboratories is difficult, if not impossible [15]. We have collected some of the results from fast redox experiments which appeared in the literature on homogeneous series of ceria–zirconia samples in the entire range of composition. By plotting the data all together (this was done by rescaling OSC values obtained in each laboratory on a common axis), a quite significant, though still qualitative relation can be obtained (Fig. 3). Two features are clearly evidenced: (i) the line behind the OSC values is a curve that clearly shows a maximum and (ii) the maximum is not narrow and can be located in the range of composition $Ce_xZr_{1-x}O_2$ with $0.5 < x < 0.8$. The main conclusions are therefore in qualitative agreement with those obtained from TPR analysis. We will briefly attempt to provide an explanation for the above features, which represent the main general outcome from redox studies (either total or dynamic experiments) on ceria–zirconia.

3.1. The origin of OSC activity

Ceria crystallizes in a cubic fluorite structure (*Fm*3*m* space group) where each cerium cation is coordinated by eight equivalent nearest-neighbour oxygen anion at the corner of a cube. The substitution of some Ce^{4+} ions for Zr^{4+} favours the formation of defects in the ceria–zirconia lattice that induces a distortion of the oxygen sublattice. This is because the ionic radius of Zr^{4+} is too small compared to that of Ce^{4+} to accom-

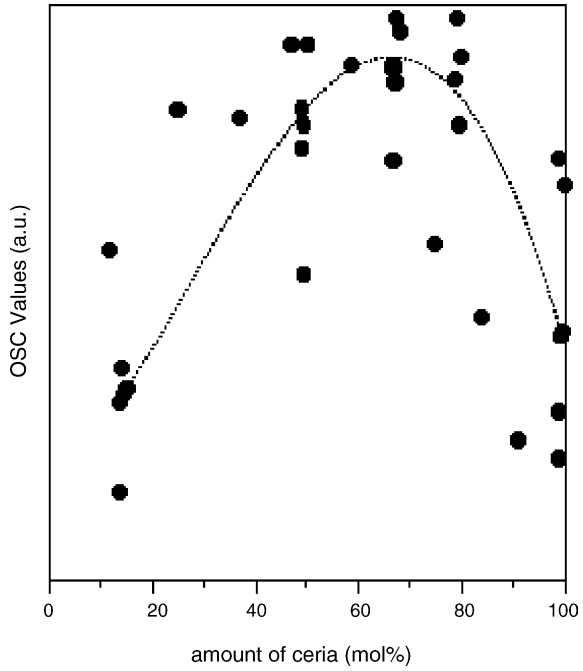

Fig. 3. OSC against ceria content in ceria–zirconia solid solutions. Data were taken from Refs. [26–31]. OSC values from the different sets of experiments were rescaled to be visualized on the same plot.

modate all the oxygen. This distortion increases with the Zr content and is responsible for the progressive change of the symmetry of solid solutions toward tetragonal $P4_2/nmc$ (t″ and t′). It is not possible to identify clearly the composition at which phase separation occurs, as this depends on several factors including sample preparation and treatment, although generally ceria-rich composition crystallizes easily with a cubic symmetry while intermediate and zirconia-rich compositions prefer a tetragonal phase. From this picture, it is expected that solid solutions having the highest concentration of Zr will show the best redox behaviour. However, this is not completely true, since a high ZrO_2 content will reduce the quantity of active redox element. Therefore, a detailed balance between structural defects and Ce content must be reached for optimum results.

One of the possible methods to quantify defects is that of calculating the position of oxygens within the lattice which in tetragonal (t′, t″) structures is shifted from ideal position observed in cubic structure. The displacement value against Ce/Zr concentration shows a maximum in the intermediate composition range [32,33]. On the other side, the amount of active redox element decreases by increasing the Zr content. Therefore, in the intermediate composition range, there is an optimum balance between amount of redox elements and number of defects and consequently OSC (both total and dynamic) versus composition plot does show a maximum.

The second question that we should answer is related to the location of the maximum. From the individual dynamic OSC measurements carried out in different laboratories the position of the maximum shifts in the range from $x \approx 0.5$ to 0.9 in $Ce_xZr_{1-x}O_2$. This highlights the sensitivity of OSC values to a number of different variables like the preparation methods, which include also pre and post-treatments of powders, the phase purity of the solid solutions, and the surface properties. The difficulty and the uncertainty of obtaining "single phase" materials has been recently highlighted [7]. The majority of materials after high-temperature treatment do show phase separation, and although the average composition is unchanged, the effect is that of having a mixture of solid solutions. It has been recently suggested that the presence of small domains (enriched in ceria and zirconia and undetectable with conventional diffraction analysis) within crystallites of $Ce_{0.5}Zr_{0.5}O_2$ and the associated interfacial area could be responsible for the increase of total OSC [25]. This is likely the reason of the difference in total OSC of the three compositionally identical samples reported in Fig. 3. On the contrary, atomically homogeneous ceria–zirconia solid solutions is believed to be the cause of increased total OSC in $Ce_{0.5}Zr_{0.5}O_2$ [34] due to the modification of the local oxygen environment around Ce and Zr, as determined by EXAFS analysis, that agrees well with explanations suggested several years ago [22]. Again, discrepancies in the outcome of the results from different laboratories derive from synthesis and treatment procedures: samples in Ref. [34] were treated under reductive atmosphere at high temperature (a procedure which is known to accelerate the ordered arrangements of cations), while samples in Ref. [25] were subjected to oxidative treatment only. In addition, in most of these studies, metal loaded samples are used to measure OSC (which might have some drawbacks related to additional effects that might interfere with OSC measured with H_2, like spillover effect, dispersion, etc., and whose effects are not clearly separated from true OSC). What clearly emerges from these advanced studies is that Ce/Zr solid solutions must be designed and studied at an atomic level in order to develop high performances and understand their key features.

4. Some implications of the redox features in catalytic applications

The redox behaviour of ceria and ceria–zirconia has a great impact on several catalytic reactions. It was reported from the early studies of Yao [35] that ceria has a beneficial effect for CO oxidation and NO*x* reduction under both stoichiometry and excess oxygen. The ability of ceria and ceria–zirconia to donate oxygens to supported metals is also a key feature in other catalytic reactions like for example, catalytic combustion [36] and water gas shift reaction [37–39].

4.1. Oxidation of CO

We have recently studied in more detail CO oxidation under both stationary and cycled feedstream conditions over

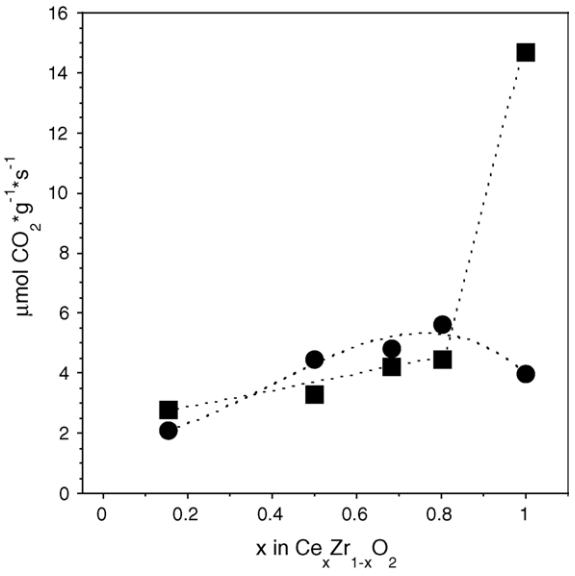

Fig. 4. Reaction rate in CO oxidation under cycling (●) and stationary (■) conditions for various composition, Ref. [31].

bare ceria and ceria–zirconia [31,40]. The results show that both ceria and ceria–zirconia are active in CO oxidation; however some relevant differences are observed depending on textural properties of samples and composition. By comparing catalysts with different composition but similar surface areas it is shown that the rate of CO_2 formation under stationary conditions is almost proportional to the amount of ceria, whereas under cycled feedstream conditions the rate reaches a maximum when CeO_2 is within the range of 50–80 mol%. In addition, while with pure ceria the rate is higher under stationary conditions, with ceria–zirconia the rate is higher under cycling conditions (Fig. 4). A decrease in surface area by ageing strongly affect reactivity under stationary conditions, while activity under cycled mode is less affected. It was also observed that in the temperature range where activation occurs, diffusion of oxygen in the bulk in solid solutions is much faster than in pure ceria, suggesting that the participation of oxygen from the bulk could contribute to the observed behaviour in the timescale of these experiments, while with ceria its participation is more critical [31,41].

A more detailed study on the mechanism of CO oxidation under cycled feedstream conditions has been undertaken in order to disclose some effects of CO/CO_2 adsorption/desorption that have been detected when studying redox behaviour of ceria and ceria–zirconia with CO [40]. It is shown that more than one process occurs on the surface during oxidation, and the rate of these processes is strongly dependent on surface area and to a lesser extent on composition. Great differences are observed between pure ceria and solid solutions, but within solid solutions the differences are less important, especially in the ceria-rich region. A mechanism to explain the main characteristics of CO oxidation has been put forward and the following simplified reaction scheme can be suggested:

$$CO_{(g)} + 2CeO_2 \rightarrow CO_{2(g)} + 2CeO_{1,5} \quad (1)$$

$$CO_{(g)} + 2CeO_2 \rightarrow CO_{2(s)}{}^{*} + 2CeO_{1,5} \quad (2)$$

$$O_{2(g)} + CeO_{1,5} \rightarrow (O_2)_{ads} - CeO_{1,5} \quad (3)$$

$$O_{2ads} \rightarrow 2O_{ads} \quad (4)$$

$$CO_{2(s)}{}^{*} + 2O_{ads} + 4CeO_{1,5} \rightarrow CO_{2(g)} + 4CeO_2 \quad (5)$$

Formation of CO_2 takes place in two distinct moments: a fraction of the CO is rapidly oxidized to CO_2 and the CO_2 desorbs readily from the catalysts (reaction (1)), while the remaining fraction of CO/CO_2 is adsorbed and slightly accumulates on the catalyst (forming carbonate like species indicated as $CO_2{}^{*}$ in reaction (2)). Its desorption is stimulated during the lean part of the cycle (reaction (3)–(5)) when oxygen is pulsed over the catalyst. Both CO_2 formation mechanisms contribute to the overall activity observed but reaction rate changes strongly with surface area and composition. The first contribution (true oxygen storage) is faster with ceria–zirconia than with ceria and not strongly dependent on surface area: the second CO_2 contribution is faster on ceria than on ceria–zirconia and strongly dependent on surface area. The overall oxidation activity is a balance between these contributions. With high surface area, catalysts similar activities are observed in all ceria-rich samples but the origin of this activity is different: while for ceria the main contribution is from reaction (2) for ceria–zirconia it mainly derives from reaction (1). In contrast, the activity of ceria–zirconia in low surface area samples is by far better than that observed on pure supports. In this case, reaction (2) is almost totally depressed and overall rate depends almost exclusively from reaction (1) which is directly connected to oxygen storage, and therefore much faster in ceria–zirconia.

4.2. Soot oxidation

Among the several techniques that have been developed for reducing particulate emissions from diesel engines, filtering followed by catalytic oxidation is one of the more promising. In the catalytic approach, the system is based on the use of a catalyst to achieve the onset of regeneration at a significantly lower temperature [42].

Regarding the intimate atomic mechanism involved in oxidation of carbon, several authors pointed out the importance of redox properties of the catalyst. That is, the effectiveness of the catalyst can be related to its ability to deliver oxygen from the lattice to the gas phase (or better to the solid carbon reactant) in a wide temperature range. Recently, it has been reported that the use of supports based on cerium oxide confers interesting properties to soot combustion catalysts due to high availability of surface oxygen and high surface reducibility [43–45]. We have therefore compared the properties of ceria and ceria–zirconia in the combustion of soot (Fig. 5). The comparison of combustion activity is based on the evalu-

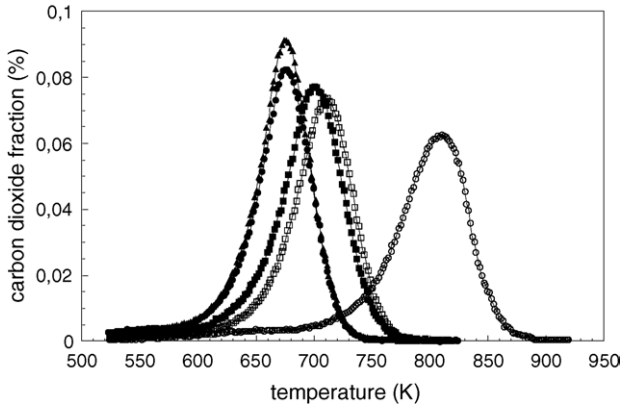

Fig. 5. TPO profile of soot combustion in samples of low surface area ceria–zirconia CeO_2 (■), $Ce_{0.75}Zr_{0.25}O_2$ (●), $Ce_{0.44}Zr_{0.56}O_2$ (▲), $Ce_{0.28}Zr_{0.62}O_2$ (□), ZrO_2 (◯). Experimental conditions: 25 mg sample (mixing ratio soot-cat. 1:20), total flow 400 ml/min, 6% O_2 in N_2, heating rate 10 K/min.

ation of the temperature of the maximum which is located at a composition between 70 and 100% of ceria for high-surface area samples and between 50 and 80% ceria for low-surface area samples. These values are depicted in Fig. 6 against composition and compared with those obtained in cycled CO oxidation. Although conditions and samples are different a similar profile is obtained in both experiments, indicating that for HSA materials activity of ceria and ceria–zirconia are comparable (in the ceria-rich region) while for LSA samples the activity of ceria–zirconia in the middle composition range is higher. This can be explained in analogy to what has been done for CO oxidation, by invoking a redox mechanism with a simple redox route for soot oxidation, which utilizes oxygen activated from the support in a typical reduction/oxidation mechanism (Mars Van Krevelen type) in which the catalyst undergoes a partial reduction (Fig. 7). Oxygen

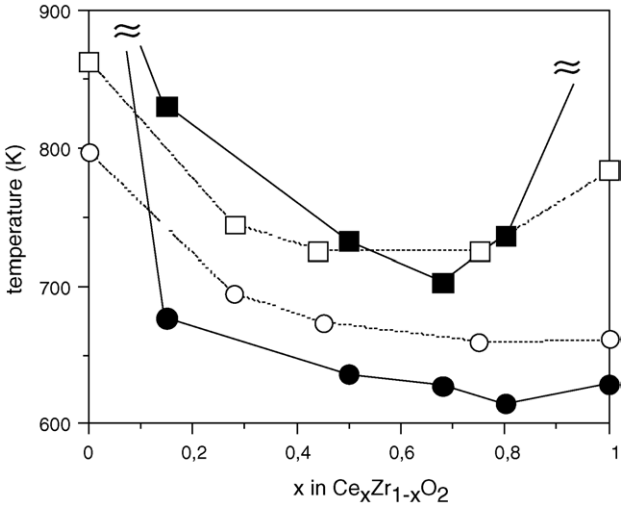

Fig. 6. Light-off temperature in CO oxidation under cycling conditions (filled symbols) and soot combustion temperature (open symbols) against composition: high surface area samples (circles), low surface area samples (squares).

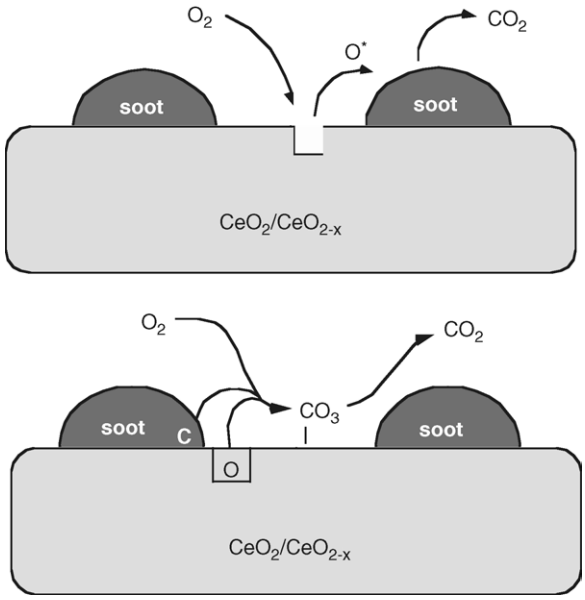

Fig. 7. Redox route (top) and carbonate route (bottom) mechanism in the CeO_2-catalyzed combustion of soot.

storage is therefore important because it provides an alternative route for the oxidation of big soot particles. An alternative redox route involve oxygen from the support and gas-phase which reacts with soot to form adsorbed CO_2 in the form of carbonates. Decomposition of carbonate is then stimulated by gas-phase oxygen which provide also reoxidation of the support.

5. Conclusions

In summary, we have shown that the understanding at an atomic level, the mechanism of ceria reduction is one of the most important steps toward the design of novel redox catalysts. The study of the redox mechanism in these materials are relevant not only for developing advanced TWC but also in the design of catalysts for applications (i.e. soot oxidation, catalytic combustion, water gas shift, ...) where participation of lattice oxygen and catalyst reducibility have shown to improve overall performances.

Acknowledgements

Authors thank MIUR (progetti PRIN) and Regine Friuli Venezia Giulia for financial support.

References

[1] A. Trovarelli (Ed.), Catalysis by Ceria and Related Materials, Imperial College Press, London, 2002, pp. 1–528.
[2] S. Bernal, J. Kaspar, A. Trovarelli (Eds.), Catal. Today 50 (2) (1999) 173–443.

[3] A. Trovarelli, C. de Leitenburg, M. Boaro, G. Dolcetti, Catal. Today 50 (1999) 353.
[4] J. Kaspar, P. Fornasiero, J. Solid State Chem. 171 (2003) 19.
[5] A. Trovarelli, Catal. Rev. Sci. Eng. 38 (1996) 439.
[6] S. Bernal, J.J. Calvino, M.A. Cauqui, J.M. Gatica, C. Larese, J.A. Perez Omil, J.M. Pintado, Catal. Today 50 (1999) 175.
[7] R. Di Monte, J. Kaspar, Top. Catal. 28 (2004) 47.
[8] V. Perrichon, A. Laachir, G. Bergeret, R. Fréty, L. Tournayan, O. Touret, J. Chem. Soc., Faraday Trans. 90 (1994) 773.
[9] G.S. Zafiris, R.J. Gorte, J. Catal. 139 (1993) 561.
[10] M.F. Johnson, J. Mooi, J. Catal. 103 (1987) 502; M.F. Johnson, J. Mooi, J. Catal. 140 (1993) 612.
[11] G. Wrobel, C. Lamonier, A. Bennani, A. D'Huysser, A. Aboukaïs, J. Chem. Soc., Faraday Trans. 92 (1996) 2001.
[12] A. Trovarelli, G. Dolcetti, C. de Leitenburg, J. Kaspar, P. Finetti, A. Santoni, J. Chem. Soc., Faraday. Trans. 88 (1992) 1311.
[13] J.E. Fallah, S. Boujana, H. Dexpert, A. Kiennemann, J. Majerus, O. Touret, F. Villain, F. Le Normand, J. Phys. Chem. 98 (1994) 5522.
[14] S. Bernal, J.J. Calvino, J.M. Gatica, C.L. Cartes, J.M. Pintado, in: A. Trovarelli (Ed.), Catalysis by Ceria and Related Materials, Imperial College Press, London, 2002, p. 85 (Chapter 4).
[15] M. Boaro, M. Vicario, C. de Leitenburg, G. Dolcetti, A. Trovarelli, Catal. Today 77 (2003) 407.
[16] A. Trovarelli, in: A. Trovarelli (Ed.), Catalysis by Ceria and Related Materials, Imperial College Press, London, 2002, p. 15 (Chapter 2).
[17] S. Bernal, J.J. Calvino, G.A. Cifredo, J.M. Rodriguez-Izquierdo, J. Phys. Chem. 99 (1995) 11794.
[18] F. Giordano, A. Trovarelli, C. de Leitenburg, M. Giona, J. Catal. 193 (2000) 273.
[19] F. Giordano, A. Trovarelli, C. de Leitenburg, G. Dolcetti, M. Giona, Ind. Eng. Chem. Res. 40 (2001) 4828.
[20] J.H. Hwang, T.O. Mason, Z. Phys. Chem. 207 (1998) 21.
[21] M. Ozawa, M. Kimura, A. Isogai, J. Alloys Compd. 193 (1993) 73.
[22] P. Fornasiero, R. Di Monte, G. Ranga Rao, J. Kaspar, S. Meriani, A. Trovarelli, M. Graziani, J. Catal. 151 (1995) 168.
[23] M. Boaro, A. Trovarelli, J-H. Hwang, T.O. Mason, Solid State Ion. 147 (2002) 85.
[24] J. Kaspar, M. Graziani, P. Fornasiero, in: K.A. Gschneidner Jr., L. Eyring (Eds.), Handbook on the Physics and Chemistry of Rare Earths, Elsevier Science B.V, Amsterdam, 2000, p. 159.
[25] E. Mamontov, R. Brezny, M. Koranne, T. Egami, J. Phys. Chem. B 107 (2003) 13007.
[26] S. Rossignol, F. Gérard, D. Duprez, J. Mater. Chem. 9 (1999) 1615.
[27] H. Vidal, J. Kaspar, M. Pijolat, G. Colon, S. Bernal, A. Cordón, V. Perrichon, F. Fally, Appl. Catal. B: Environ. 27 (2000) 49.
[28] J.-P. Cuif, G. Blanchard, O. Touret, A. Seigneurin, M. Marczi, E. Quéméré, SAE Paper 970463 (1997) 1.
[29] M. Hirano, A. Suda, J. Am. Ceram. Soc. 86 (2003) 2209.
[30] A. Trovarelli, F. Zamar, J. Llorca, C. de Leitenburg, G. Dolcetti, J. Kiss, J. Catal. 169 (1997) 490.
[31] M. Boaro, C. de Leitenburg, G. Dolcetti, A. Trovarelli, J. Catal. 193 (2000) 338.
[32] S. Enzo, R. Frattini, F. Delogu, A. Primavera, A. Trovarelli, J. Mater. Res. 15 (2000) 1538.
[33] M. Yashima, S. Sasaki, Y. Yamaguchi, M. Kakihana, M. Yoshimura, T. Mori, Appl. Phys. Lett. 72 (1998) 182.
[34] Y. Nagai, T. Yamamoto, T. Tanaka, S. Yoshida, T. Nonaka, T. Okamoto, A. Suda, M. Sugiura, Catal. Today 74 (2002) 225.
[35] H.C. Yu Yao, J. Catal. 87 (1984) 152.
[36] S. Colussi, C. de Leitenburg, G. Dolcetti, A. Trovarelli, J. Alloys Compd. 374 (2004) 387.
[37] S. Hilaire, X. Wang, T. Luo, R.J. Gorte, J. Wagner, Appl. Catal. A: Gen. 258 (2004) 271.
[38] X. Qi, M. Flytzani-Stephanopoulos, Ind. Eng. Chem. Res. 43 (2004) 3055.
[39] G. Jacobs, P.M. Patterson, L. Williams, E. Chenu, D. Spark, G. Thomas, B.H. Davis, Appl. Catal. A: Gen. 262 (2004) 177.
[40] M. Boaro, F. Giordano, S. Recchia, V. Dal Santo, M. Giona, A. Trovarelli, Appl. Catal. B: Environ. 52 (2004) 225.
[41] A. Trovarelli, M. Boaro, E. Rocchini, C. de Leitenburg, G. Dolcetti, J. Alloys Compd. 374 (2004) 387.
[42] B.A.A.L. van Setten, M. Makkee, J.A. Moulijn, Catal. Rev. Sci. Eng. 43 (2001) 489.
[43] M.L. Pisarello, V. Milt, M.A. Peralta, C.A. Querini, E.E. Miro', Catal. Today 75 (2002) 465.
[44] E.E. Miro', F. Ravelli, M.A. Ulla, L.M. Cornaglia, C.A. Querini, Catal. Today 53 (1999) 631.
[45] G. Neri, G. Rizzo, S. Galvagno, M.G. Musolino, A. Donato, R. Pietropaolo, Thermochim. Acta 381 (2002) 165.